

Measurement of Panofsky Ratio: Nuclear Absorption of π^- from K Shell in Hydrogen*

J. FISCHER, R. MARCH, AND L. MARSHALL

The Enrico Fermi Institute for Nuclear Studies, The University of Chicago, Chicago, Illinois

(Received July 12, 1957)

The ratio of charge exchange to radiative capture in hydrogen for stopped π^- mesons has been determined by measuring the total photon spectrum in a lead glass Čerenkov counter. The ratio was found to be 1.87 ± 0.10 . Possible contribution from in-flight pions has been shown to be quite small. The error has been estimated including this effect, as well as errors related to total number of events observed, and errors arising in the data analysis. Evidence for high-energy photon production by capture of slow π^- in elements other than hydrogen is discussed.

INTRODUCTION

THE Panofsky ratio, defined as the relative probability of charge exchange to radiative capture after absorption of a negative pion from the K shell in hydrogen,

$$P = \frac{\text{rate } (\pi^- + p \rightarrow \pi^0 + n)}{\text{rate } (\pi^- + p \rightarrow \gamma + n)},$$

has been measured as 0.94 ± 0.30 by Panofsky, Aamodt, and Hadley,¹ as 1.60 ± 0.17 by Kuehner, Merrison, and Tornabene,^{2,3} as 1.50 ± 0.15 by Cassels, Fidecaro, Wetherall, and Wormald,³ and as 1.10 ± 0.50 by Lederman *et al.*⁴ The present experiment has yielded a value of 1.87 ± 0.10 .

The pions used in the first-mentioned measurement were of all energies produced from an internal target hit by 350-Mev protons, and the photons were measured with a pair spectrometer. The next two measurements were made with external beams of pions slowed to thermal energies and stopped in liquid hydrogen targets. Merrison *et al.* also measured the resulting photons with a pair spectrometer, but Cassels and his colleagues used a large lead glass Čerenkov counter to observe the photon spectrum. The report of Cassels *et al.* gives a useful bibliography of experiments related to these reactions.

The present measurement was made with a glass Čerenkov counter, using a procedure similar to that of Cassels *et al.* but with some differences. In particular, the measured photons were one-hundred percent converted in the glass itself, instead of being converted by a smaller efficiency in a piece of lead in front of the

glass. In this way a correction for efficiency of conversions in the lead has been avoided. Furthermore, there was observed a background effect presumably caused by pions absorbed in the walls of the liquid hydrogen container, which was demonstrably different in the presence and in the absence of liquid hydrogen, accordingly as more or fewer pions were scattered into the walls. The magnitude of this effect was determined and corrected for by a substitution method. In the present experiment, such a large number of events were observed that the error related to the number of observations has become almost negligible. Finally in the present measurement it has been proved that the Panofsky ratio measured here is truly that of pions captured from mesonic orbits around protons; that is, small upper limits for contribution by pions in flight have been experimentally determined both for the radiative capture and for charge exchange processes.

An important property of the Panofsky ratio is the fact that it connects the ratio, R_{π} , of π^- to π^+ photo-production, with the difference of the s -wave phase shifts for the $\frac{3}{2}$ and the $\frac{1}{2}$ isotopic spin states of the $\pi^- + p$ system. The argument is briefly as follows.⁵

For pions captured by a proton from a K -mesonic orbit the p -wave phase shifts are negligible and the charge exchange cross section may be written

$$\sigma_0 \equiv \sigma(\pi^- + p \rightarrow \pi^0 + n) = \frac{8\pi}{9} \chi^2 (\delta_3 - \delta_1)^2 \frac{v_{\pi^0}}{v_{\pi^-}},$$

where v_{π^-} and v_{π^0} are the barycentric (center-of-mass system) velocities of charged and neutral pions. With $\hbar/\mu c = 1.41 \times 10^{-13}$ cm, and⁶ $(\delta_3 - \delta_1)/\eta = (\alpha_3 - \alpha_1) = 0.27$, which last amount should be corrected for isotopic spin nonconservation by an uncertain amount,⁷

$$\sigma_0 = 4.07 \times 10^{-27} \frac{v_{\pi^0}}{v_{\pi^-}}.$$

⁵ H. L. Anderson and E. Fermi, Phys. Rev. **86**, 794 (1952).

⁶ A. Roberts and J. Timlot, Phys. Rev. **90**, 951 (1953); see also J. Orear, Nuovo cimento **4**, 856 (1956).

⁷ H. P. Noyes, Phys. Rev. **101**, 320 (1956).

* Research supported by a joint program of the Office of Naval Research and the U. S. Atomic Energy Commission.

¹ Panofsky, Aamodt, and Hadley, Phys. Rev. **81**, 565 (1951).

² Kuehner, Merrison, and Tornabene, see *Proceedings of the CERN Symposium on High-Energy Accelerators and Pion Physics, Geneva, 1956* (European Organization of Nuclear Research, Geneva, 1956), Vol. 2, p. 241 for description of apparatus. Revised value of Panofsky ratio reported in 3.

³ Cassels, Fidecaro, Wetherall, and Wormald (to be published).

⁴ Beneventano, Stoppini, Tau, and Bernardini, *Proceedings of the CERN Symposium on High-Energy Accelerators and Pion Physics, Geneva, 1956* (European Organization of Nuclear Research, Geneva, 1956), Vol. 2, see footnote p. 263; see also Beneventano, Bernardini, Carlson-Lee, and Tau, Nuovo cimento **4**, 323 (1956).

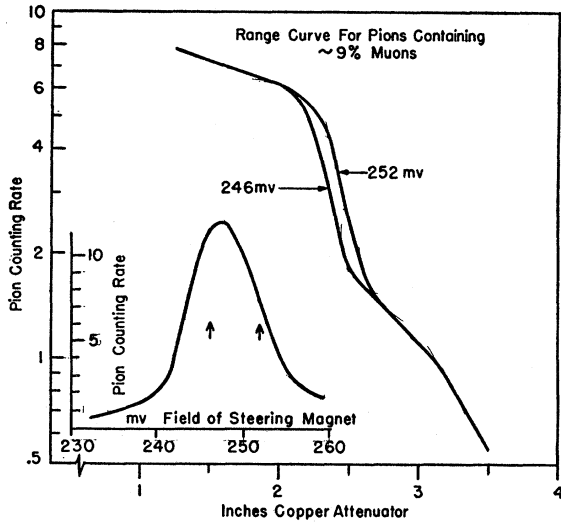


FIG. 1. Range of nominal 120-Mev π^- mesons versus thickness of copper shown for two different field values of the steering magnet.

But σ_0 is related to the Panofsky ratio P through the equation

$$\sigma(\pi^- + p \rightarrow \pi^0 + n) = P \times \sigma(\pi^- + p \rightarrow \gamma + n).$$

By use of detailed balance the right-hand side becomes

$$P \times \frac{2p_\gamma^2}{p_\pi^2} \times \sigma(\gamma + n \rightarrow p + \pi^-),$$

which is a function of R , defined as

$$R_{\mp} = \frac{\sigma(\gamma + n \rightarrow \pi^- + p)}{\sigma(\gamma + p \rightarrow \pi^+ + n)} \approx \frac{\sigma(\gamma + d \rightarrow \pi^- + 2p)}{\sigma(\gamma + d \rightarrow \pi^+ + 2n)}$$

We introduce R_{\mp} together with the measured π^+ photoproduction cross section⁴

$$\sigma(\gamma + p \rightarrow \pi^+ + n) = (1.43 \pm 0.02) \times 10^{-28} \eta,$$

and also the barycentric $p_\gamma = \mu c(1 + \mu/2M)/(1 + \mu/M)$ at threshold, and find

$$PR_{\mp} = \frac{1.407 \times 10^{-27} v_{\pi^0} (1 + \mu/M)^2}{2.143 \times 10^{-28} c (1 + \mu/2M)^2}$$

Using⁸ $v_{\pi^0}/c = 0.20$, we find $PR_{\mp} = 3.26$. The value of R_{\mp} calculated from dispersion theory is 1.34, which requires $P = 2.43$. The measured values⁴ of R_{\mp} when extrapolated to zero energy give a value of about 2, but there is some question as to whether the extrapolation as presently done is meaningful. Moravcsik⁹ has discussed many of the uncertainties inherent in the extrapolation. A value of R_{\mp} of about 2 is in agreement with the ratio P measured by Cassels *et al.*³ and by us.

⁸ W. Chinofsky and J. Steinberger, Phys. Rev. **93**, 586 (1954).

⁹ M. J. Moravcsik, Nuovo cimento (to be published).

EXPERIMENTAL

A beam of 120-Mev π^- from the cyclotron after magnetic analysis was slowed through that amount of attenuator corresponding to the inflection point on the range curve (Fig. 1), made up of ~ 2 -in. copper, followed by two monitor plastic scintillation counters, 1 and 2, each of $\frac{1}{4}$ -in. thickness CH_2 , and then followed by 1-in. polyethylene plus $\frac{1}{8}$ -in. copper. The full energy width of the pion beam was 7 Mev. The diameters of counters 1 and 2 were 6 in. The pions next passed into a liquid hydrogen container or various other targets. Photons emitted at 90° to the pion beam direction passed through a collimator in a Pb wall 8 in. thick into a Corning Pb glass Čerenkov counter, protected by a scintillation plastic anticoincidence counter, 3.

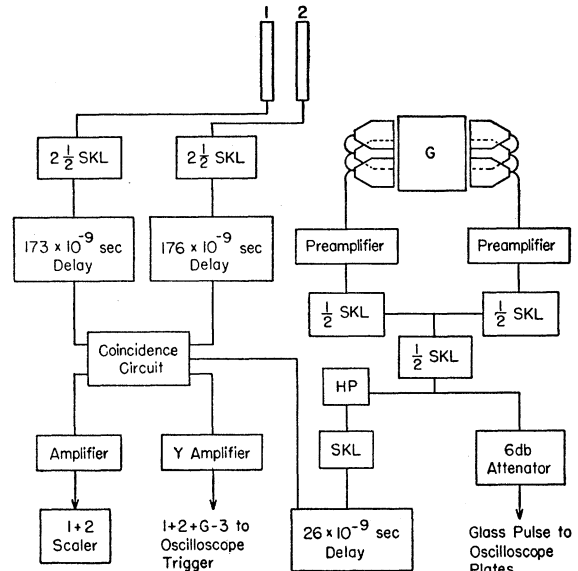


FIG. 2. Block diagram of basic components of counting apparatus. HP means Hewlett Packard distributed amplifier 460A, and SKL means Spencer Kennedy Laboratory 202D distributed amplifier. G designates Pb glass Čerenkov counter adjoining 5819 DuMont phototubes indicated schematically.

The glass counter ($d = 3.89$, $n = 1.649$ for NaD) was made of a cylinder of glass 7 in. high by 12-in. diameter. On each of the flat sides were mounted three DuMont photomultipliers of 5-in. diameter connected optically to the glass by a glycerine seal. The six photomultipliers were selected for equality of pulse height response to a test source. The glass and the photomultipliers were protected from stray magnetic fields by two concentric outer cylinders of μ metal, each 0.02 in. thick and separated by a $\frac{1}{4}$ -in. fiber shell between the μ -metal shells.

Photons passing through the collimator in the Pb wall entered the glass cylinder through the curved surface. The pulses from the photomultipliers were adjusted to be equal for the case when monoenergetic electrons from the 100-Mev betatron were fed into the

glass, and at the same time the delays in the various photomultipliers were adjusted so that the 6 pulses arrived at an external point simultaneously, i.e., within 1×10^{-8} second.

A block diagram of the electronics is shown in Fig. 2. The main feature is that the combined pulse from the glass counter was split, with half going to make a coincidence with the 2 monitor counters 1 and 2 together with counter 3 in anticoincidence. The output of the coincidence circuit triggered the oscilloscope sweep, upon which was displayed the other half of the pulse from the glass counter and which was recorded photographically.

The electronic variables were adjusted with electron beams from the betatron, and the efficiency was measured as a function of electron energy for a collimated beam of monoenergetic electrons passing through counters 1 and 2 and going into the glass counter. The efficiency curve, measured as the rate of triple coincidences, $1+2+glass$, divided by rate of double coincidence, $1+2$, versus energy of electron beam, is shown in Fig. 3. For 96 Mev, 70 Mev, and also for

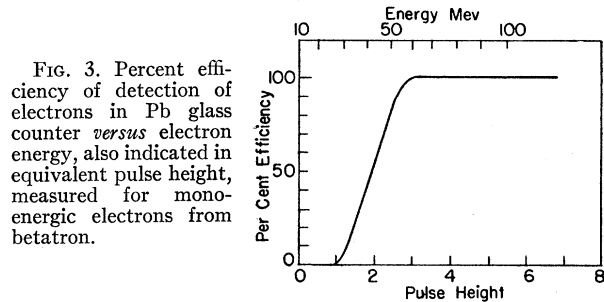


FIG. 3. Percent efficiency of detection of electrons in Pb glass counter versus electron energy, also indicated in equivalent pulse height, measured for monoenergetic electrons from betatron.

43-Mev electrons (selected by a magnet) the pulses from the glass were photographed on the oscilloscope sweep, and the pulse heights were read off the film in projection. In this way the efficiency curve previously found versus energy of the electrons was related to height of pulse from the glass counter, and at the same time the resolution of the glass counter was determined as a function of energy (Fig. 4).

In spite of extensive heavy concrete shielding around the glass counter in the cyclotron experimental area, there was a large random background count, apparently caused by neutrons and present only when the cyclotron was running. The spectrum of the background was measured as a function of gain of the amplifier which fed the oscilloscope sweep trigger with the pulse from the coincidence circuit. For high gain the dependence of the logarithm of oscilloscope trigger rate versus pulse height was found to be linear, but to depart from linearity with decreasing gain at low pulse heights. The ratio of the curve for gain 0.065 (namely that used in the present measurements) to the curve for gain 0.09 (Fig. 5), gave a second measure of the efficiency of the

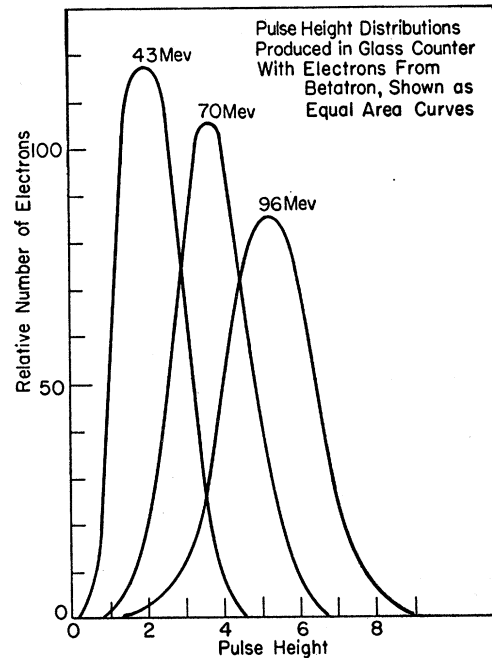


FIG. 4. Pulse-height resolution curves for glass counter measured by using 43-, 70-, and 96-Mev electrons from betatron.

glass counter through the region 30-60 Mev in good agreement with that measured using electrons from the betatron. This confirmation indicated that the efficiency of the glass counter did not depend too sensitively on the position in the glass where the Čerenkov light was created, showing an equivalence between, on the one hand, betatron electrons which begin to emit light as they enter the glass and on the other hand, light from radiation whose source was the general room background and which might be created at any arbitrary point in the glass.

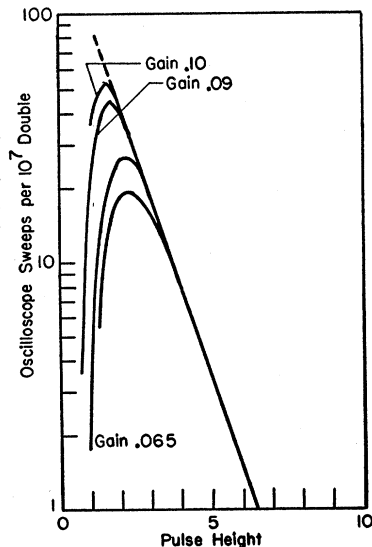


FIG. 5. Gain in Y amplifier which controlled the height of pulse to trigger the oscilloscope sweep versus pulse-height spectrum in glass counter measured with cyclotron turned on. This background was presumably caused by a general flux of neutrons which managed to penetrate a large amount of shielding.

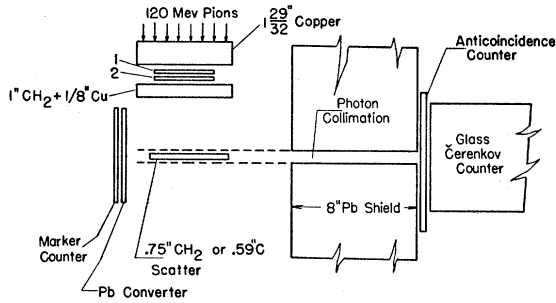


FIG. 6. Schematic drawing of geometry for measurement of pulse-height spectrum from CH_2 , carbon, and other elements. Measurements were made both with and without marker counter. For measurements with marker counter, an anticoincidence counter not shown above was imposed between Pb converter and target.

MEASUREMENTS WITH CH_2 AND C

It was observed and explained by Panofsky, Aamodt, and Hadley¹ that if H atoms are in the presence of nuclei of higher Z , incident negative thermal pions are absorbed, as far as can be detected, only by the nuclei of higher Z . This follows because although the π -H atom may form, its life is long compared with the time for collision with other nuclei, and therefore the probability is large for capture of the pion onto the nucleus with higher Z .

This fact allows an upper limit to be determined for charge exchange by those pions in the beam which do not come to rest in a hydrogen target. Such a limit was needed because the hydrogen target was thin compared with the energy width of the beam, the thickness of liquid hydrogen subtended by the photon collimator being 3 inches or $\sim \frac{1}{2}$ gram of hydrogen which stopped or scattered out approximately 30% of the incident pions.

The upper limit to charge exchange by in-flight pions was measured by observing the pulse spectrum in the glass counter produced by pions in CH_2 , and observing in particular those pulses in the glass which were produced in coincidence with a pulse in a large plastic scintillator ("marker" counter) placed behind a $\frac{1}{2}$ -in. Pb converter, opposite to the glass counter. A large plastic scintillator counter in front of the lead converter and in anticoincidence with the marker counter prohibited the counting of charged particles. The argument is that, because all pions coming to rest, even those forming $\text{H}\pi^-$, will be captured by C instead of H nuclei and will not produce π^0 , the two coincident

photons from π^0 decay can be produced only by in-flight pions. Therefore the maximum observed number of these events determines an upper limit for the charge-exchange contribution on H by the in-flight component of the slow pion beam. It is important to determine this limit because, as has been pointed out by Bernardini,¹⁰ the observed Panofsky ratio might be substantially changed by a non-negligible in-flight contribution.

The geometry is shown schematically in Fig. 6. Targets of 0.75 in. \times 5 in. width CH_2 and of 0.59 in. \times 5 in. carbon were placed within the umbra of the photon collimator. The average vertical dimension of the scatterer viewed by the collimator was 2.5 inches. If a pulse in the marker counter coincided with one in the glass counter pulse, the marker counter pulse appeared on the oscilloscope sweep after the glass pulse, marking it as one produced as if from the decay of a π^0 . Both for the CH_2 and for the C target, the rate observed for marked pulses was not significantly different from the rate observed with no target at all within the limits of statistical error.

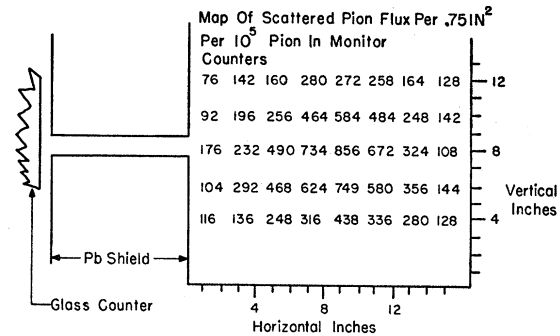


FIG. 7. Map of thermal pions measured in plane of photon collimator at a distance 7 in. from attenuator. The pion distribution was produced by attenuating a 120-Mev π^- beam to the inflection point of its range curve.

The net rate observed for $(\text{CH}_2 - \text{BG})$, where BG is the background, is shown in Table I. The marker counter was 8.6 in. \times 10.7 in. and was 6 in. away from the center of the scatterer. It was estimated, taking into account the volumes of liquid hydrogen and of CH_2 scatterer in the umbra and in the penumbra of the collimator and taking into account the relative pion fluxes (see Fig. 7) on the various volumes, that effectively the ratio of number of atoms of H in liquid hydrogen to that in the CH_2 target was 1.76. The production of π^0 by in-flight pions to photons from liquid hydrogen then was estimated to be

$$\leq \frac{2.2 \pm 1.4}{10^7 \text{ pions}} \times 1.76 = \frac{3.9 \pm 2.5}{10^7 \text{ pions}},$$

where 0.5 is the efficiency of the Pb converter covering the marker counter.

TABLE I. Estimate of in-flight-contribution using marker pulses from $(\text{CH}_2 - \text{BG})$.^a

Markers/double	Attenuator	Collimation	Corrected for efficiency of converter
$(3-2)/4.2 \times 10^6$	2 $\frac{3}{8}$ -in. copper	1 in. \times 2 in.	$(2.7 \pm 6.7)/10^7$
$(16-8)/36 \times 10^6$	2 $\frac{1}{4}$ -in. Cu + 1-in. CH_2	$\frac{3}{4}$ in. \times $\frac{3}{4}$ in.	$(2.9 \pm 1.8)/10^7$

^a BG means background.

¹⁰ G. Bernardini (private communication).

A second estimate of the same quantity was made in a different way without using the marker counter. Namely, the spectra of glass pulses from targets of CH_2 (0.75 in. \times 5 in.) and C (0.59 in. \times 5 in.), having approximately equal stopping power, were photographed and measured. Figure 8 shows the respective pulse height spectra, with background subtracted, *versus* energy, and in Table II are given the total observed net counts per pion from pions in flight hitting H atoms. In liquid hydrogen, then, the upper limit to charge exchange plus radiative capture is

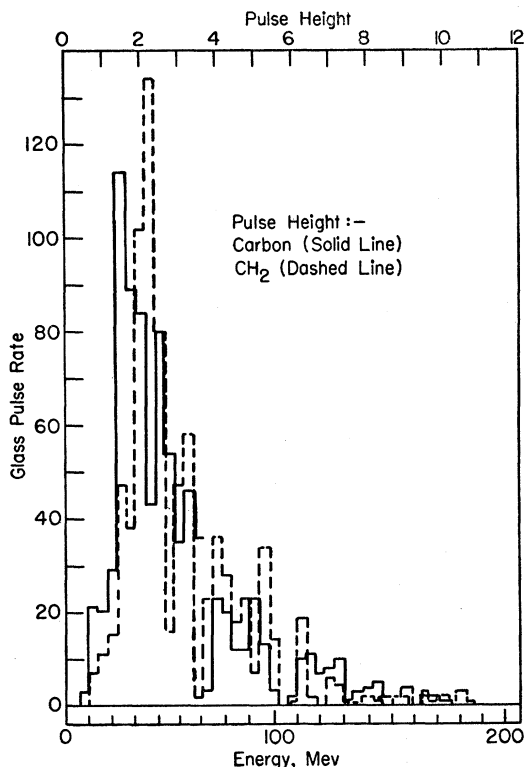


FIG. 8. Pulse-height spectra in glass counter for CH_2 and C targets having same stopping power. Ordinate is given as total counts for $\frac{1}{4}$ pulse-height interval for 4.33×10^6 pions in counters 1 and 2.

estimated as

$$(5 \pm 6.5) \times 1.76 / 10^7 = (8.8 \pm 11.4) / 10^7 \text{ pions}$$

when one uses the data of Table II. The total number of pulses above 100 Mev shown in Fig. 8, namely those which could be related to radiative capture in flight, are

$$(0 \pm 3.5) \times 1.76 / 10^7 = (0 \pm 6.2) / 10^7,$$

and those below 100 Mev which may be related to charge exchange in flight on hydrogen nuclei are

$$(5 \pm 5.5 \times 1.76 / 10^7 = (8.8 \pm 9.7) / 10^7.$$

For the measurement with hydrogen the geometry is shown schematically in Fig. 9. The liquid hydrogen

TABLE II. Yields of photons from thermal π^- captured in C and in CH_2 .

$\{[\text{CH}_2 - \text{BG}] - 0.63[\text{C} - \text{BG}]\}$	Photon collimation	Pion attenuator
$(17 \pm 12) / 10^7$	$1\frac{1}{4}$ -in. \times $1\frac{1}{4}$ in.	$2\frac{1}{2}$ -in. Cu + 1-in. CH_2
$(+3 \pm 11) / 10^7$	$\frac{1}{2}$ -in. \times $\frac{1}{2}$ in.	$2\frac{1}{2}$ -in. Cu + 1-in. CH_2
$(+21 \pm 18) / 10^7$	$\frac{1}{2}$ -in. \times $\frac{1}{2}$ in.	$2\frac{1}{2}$ -in. Cu + 1-in. CH_2
$(5 \pm 13) / 10^7$	$\frac{1}{2}$ -in. \times $\frac{1}{2}$ in.	$2\frac{1}{2}$ -in. Cu + 1-in. CH_2
$(-4 \pm 15) / 10^7$	$\frac{1}{4}$ -in. \times $\frac{3}{4}$ in.	$2\frac{1}{2}$ -in. Cu
$(+5 \pm 6.5) / 10^7$ Average		
liq. H: $(780 \pm 5) / 10^7$		Net: $(595 \pm 5) / 10^7$
BG: $(185 \pm 2) / 10^7$		

Styrofoam container had inside dimensions 14 in. long in the direction of the collimator by 5 in. wide in the direction of the incident pion beam. The center of the pion beam was 6 in. from the Styrofoam wall nearest to the collimator. The pulse-height spectrum observed for hydrogen plus container and for the container alone are shown in Fig. 10. It was observed early in the course of this experiment that there was a component of the pulse height spectrum which depended on the shape of the container and also on the presence of liquid hydrogen in the container in such a way as if produced by capture of pions scattered into the walls by the liquid hydrogen. The effect could be greatly amplified by putting pieces of wall material into the liquid hydrogen. In order to determine the correct background to subtract from the spectrum of hydrogen plus container, background spectra were measured for the empty container as a function of thickness of sheets of polyethylene scatterer placed as shown in Fig. 9, in the pion beam, but out of the view of the glass counter. In this position the polyethylene sheet simulated the effect of liquid hydrogen in scattering pions into the walls of the container. The background counting rate as a function of polyethylene sheet thickness is shown in Fig. 9. The rate at first increases rapidly and then apparently

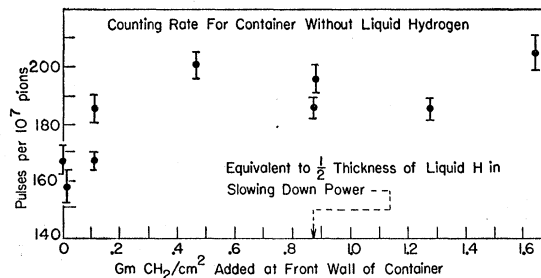
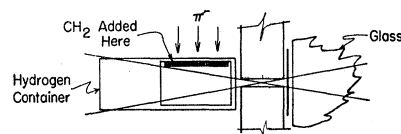


FIG. 9. Schematic drawing of geometry used with large styrofoam hydrogen container, and also background counting rate for empty container *versus* thickness of CH_2 scatterers simulating scattering and attenuation effects of liquid hydrogen.

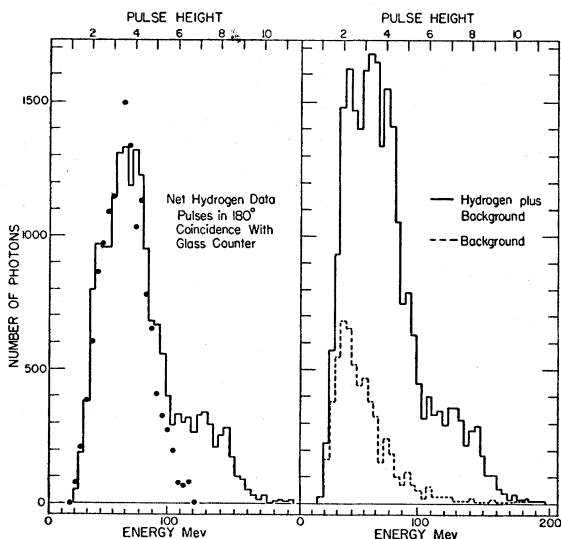


FIG. 10. Pulse-height spectra in glass counter for container plus liquid hydrogen, for empty container, and net spectrum. Ordinate is total pulses per $\frac{1}{4}$ pulse height unit per 31.8×10^7 pions in counters 1 and 2.

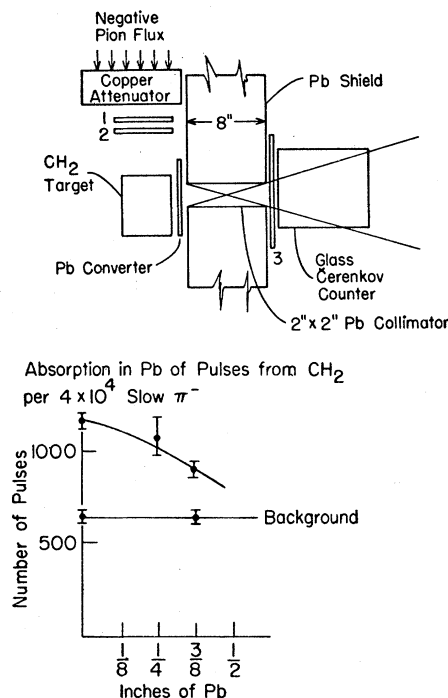
reaches a saturation value. This is the value to which the spectrum of the empty container was normalized before subtraction from the spectrum of hydrogen plus container. This saturation effect is probably due to the fact that for very low energy pions the root-mean-square multiple scattering angle $\langle \theta^2 \rangle_{Av}^{\frac{1}{2}}$ quickly approaches 180° , and the distribution of scattered slow π^- in the container approaches isotropy. Because calculations of $\langle \theta^2 \rangle_{Av}$ indicated that such a situation prevailed in the liquid hydrogen, it followed that the saturation value was the most realistic estimate of background. The counting rates are listed in Table II for liquid hydrogen plus container, for empty container thus normalized, and the difference of the two, presumed to be the net contribution of the liquid hydrogen. Note that in the net spectrum the contributions of charge exchange and radiative capture are not separated. The separation was performed by a method similar to that described by Cassels *et al.*¹¹ The shape of the π^0 contribution was determined by the marker pulse technique. A small Styrofoam container for liquid hydrogen was used, having a trapezoidal cross section of internal width 8 in. The center of the beam was 5 in. from the internal wall adjoining the collimator and 3 in. from the opposite wall. The marker counter was 6 in. from the center of the pion beam and had dimensions 8.6 in. \times 10.7 in. The marker spectrum is shown as the black spots in Fig. 10. This spectrum was corrected for the variation with photon energy of the efficiency of the Pb converter, taking into account that in coincidence with a photon of greater than $\frac{1}{2}m_\pi c^2$ in the glass there must be a

photon of less than $\frac{1}{2}m_\pi c^2$ in the marker counter. The Doppler-broadened photon spectrum for the π^0 decay was calculated for this purpose in the usual way. The corrected marker spectrum was fitted to the net hydrogen spectrum by calculating the proportionality factor

$$\alpha = \frac{\sum_0^X H(x)M(x)}{\sum_0^X M(x)^2},$$

where $H(x)$, $M(x)$ are the total number of counts of pulse height x for the net-hydrogen and for the marker spectra, respectively. The limit X was chosen to lie in the region of pulse height just below the point at which the radiative capture might begin. Below X , the net hydrogen spectrum was assumed to be exclusively due to charge exchange, and above X the difference $H(x) - \alpha M(x)$ was interpreted as radiative capture, and $\alpha M(x)$ was taken as charge exchange. In this way errors in determining α affect only the data between X and the point at which $M(x)$ effectively vanishes, which are less than 20% of the total data.

Sensitivity of the Panofsky ratio to choice of X was tested, and it was found that varying X within the limits 3.75 to 5.25 on our pulse-height scale changed R only by $\pm 1.1\%$. Choosing a value $X=4.5$, we obtained $R=1.88$.



¹¹ J. M. Cassels, *Proceedings of the Sixth Annual Rochester Conference on High-Energy Physics, 1956* (Interscience Publishers, Inc., New York, 1956).

FIG. 11. Schematic geometry for observation of attenuation in Pb of radiation from slowed π^- capture in CH_2 , and also Pb attenuation curve.

The known errors inherent in the determination may now be listed: (1) the statistical counting error for π^0 events which depends on the total number of events including background, 25 460, and on $\alpha^2 \int_x^\infty M dx = 33\ 800$ (to take into account the error caused by a limited number of marker events) and is given by $[(25\ 460 + 33\ 800)/14\ 876]^{1/2} = \pm 1.6\%$ where 14 876 is the number of net π^0 events; (2) the statistical counting error for radiative capture events which depends on the total number of events including background, 5115, and again on $\alpha^2 \int_x^\infty M dx = 33\ 800$, and is given by $(5115 + 33\ 800)^{1/2}/3935 = \pm 5.0\%$, where 3935 is the number of net radiative capture events; (3) choice of limit X in least-squares fit, $\pm 1.0\%$; (4) π^0 production by in-flight pions, $-0.7 \pm 0.4\%$ on numerator; (5) radiative capture by in-flight pions, $0 \pm 1.0\%$ on

TABLE III. Relative yields.

Targets at 45° to incident pion flux and cover- ing collimator aperture	Measured photons per 10^7 pions	Effective grams/cm ² at 5 Mev	$-dE/dx$ (Mev/g cm ²)	$(\frac{dE}{dx}) \Delta x$ Mev	Relative yield
59-in. carbon	35 ± 4	1.69	73	123	1
$\frac{1}{2}$ -in. aluminum	23 ± 11	2.42	60	145	0.56 ± 0.11
$\frac{3}{8}$ -in. copper	37 ± 7.4	3.01	47	141	0.92 ± 0.21
$\frac{1}{4}$ -in. lead	31 ± 7.4	2.56	30	76.8	1.42 ± 0.37
Hydrogen	595 ± 5	0.90	174	156.6	20*

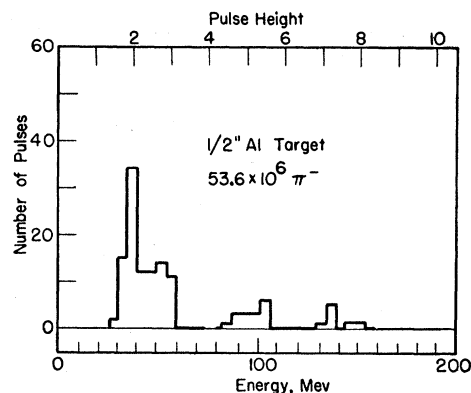
* Corrected for lower average pion flux incident on hydrogen.

denominator. Then it follows that $R = 1.88(1 - 0.007) = 1.87$, with a percentage error of

$$\{(1.6)^2 + (5.0)^2 + (1.0)^2 + (0.7)^2 + (1.0)^2\}^{1/2} = 5.5\%,$$

corresponding to $R = 1.87 \pm 0.10$.

Some investigation was made into the nature of the radiation creating the pulses in the glass counter from pions scattered into and absorbed into the walls of the hydrogen container. To this end, a few Pb absorption measurements were made (see Fig. 11) for radiation from a CH_2 target, which suggest that a large part of the radiation consists of photons. Relative yields of radiation for various elements are given in Table III, normalized to approximately equal stopping power, and compared to the yield from carbon. According to these data the probability to produce this radiation,

FIG. 12. Pulse-height spectrum from slowed π^- capture in Al.

upon capture of a π^- into nucleus, is roughly independent of Z of the nucleus.

Finally some scanty data of the pulse-height spectrum for pions absorbed in aluminum are shown in Fig. 12. One sees in Figs. 8 and 12 that the pulses range with rapidly decreasing probability to the full energy of the pion mass. The solid angle of observation was 5.2×10^{-3} steradian, and the intensity factor between pion counting rate in monitor counters and pions stopped in the target is about 5. The observed rate of emission of radiation is therefore about 3% per stopped pion. Estimates for intensities of electromagnetic processes in nuclei excited by slow π^- absorption, e.g., nucleon-nucleon bremsstrahlung, fall short by about an order of magnitude. We have been able to think of no very good explanation, but it is perhaps not inappropriate to suggest an enhancement of such processes by the cooperative action of adjacent nucleons, for example bremsstrahlung processes with virtual deuterons, alpha particles, and all other nuclear aggregates possible in the nucleus.

ACKNOWLEDGMENTS

We are grateful to Hans Kobrak, J. Kim, and Richard Worley for help with experimental arrangements, and to Charles Oxley for a kind generosity with betatron facilities. We profited by many discussions with Y. Nambu, M. L. Goldberger, and V. Telegdi.